Robotics and Autonomous Systems 74 (2015) 184–194

Contents lists available at ScienceDirect

Robotics and Autonomous Systems

journal homepage: www.elsevier.com/locate/robot

Research on the implementation of average speed for a bionic robotic dolphin

Ren Guang [a,*], Dai Yaping [a], Cao Zhiqiang [b], Shen Fei [c]

[a] School of Automation, Beijing Institute of Technology, Beijing 100081, PR China

[b] The State Key Laboratory of Management and Control for Complex Systems, Institute of Automation, Chinese Academy of Science, Beijing 100190, PR China

[c] Research Center of Precision Sensing and Control, Institute of Automation, Chinese Academy of Science, Beijing 100190, PR China

HIGHLIGHTS

- A new concept of KEMC is proposed for the forward locomotion of robotic dolphin.
- An engineering KEMC equation is established by fitting the oscillating tail.
- A data-driven method implements the average forward speed for the robotic dolphin.

ARTICLE INFO

Article history:
Received 20 January 2015
Received in revised form
14 July 2015
Accepted 20 July 2015
Available online 28 July 2015

Keywords:
Robotic dolphin
KEMC
Average speed
Iterative learning identification
Adaptive control

ABSTRACT

This study proposes an average propulsive speed implementation approach for robotic dolphins theoretically and experimentally. First, it analyzes the motion feature of the robotic dolphin, and finds the strictly corresponding rule between tail's oscillating frequency and propulsive speed of robotic dolphin. A kinetic energy mapping coefficient (KEMC) is defined to extract the motion feature. Then, it establishes a kinematic feature equation based on the KEMC definition. The feature equation takes the KEMC as a feature data, and describes a kinetic energy mapping relation for robotic dolphin's motion. Furthermore, by applying the feature equation and KEMC data, it designs an iterative learning identification and adaptive control solution to adjust automatically the average propulsive speed. Simulations prove the system's convergence and speed adjustment effectiveness. Experiments have been performed in two steps. One, a series of KEMC values are identified through the offline identification, and the distribution of KEMCs is partially known; second, a closed loop control experiment reaches the expected speed target. This study shows that the average speed implementation method based KEMC converts the speed control issue into one kind of pure control problem, and it helps robotic dolphin obtain learning ability and adaptive ability.

1. Introduction

The dolphin is a type of whale, but it is usually regarded as a fish in research of its propulsive mode. The dolphin swims quickly and very efficiently, and it is an ideal bionic object for underwater vehicles. Lots of researchers make a series of achievements in hydrodynamic, dynamic modeling and locomotion control.

In terms of hydrodynamics, there are some typical research achievements. Bose [1] adopted two-dimensional aerofoil theory to model cetaceous caudal fins, and further calculated hydrodynamic performance. Nakashima [2] proposed a method to analyze the hydrodynamic performance of robotic dolphins with two joints. Weihs [3] studied the situation in which a small dolphin swims following a large dolphin, and described the process of leaping out of the water in detail. Barrett [4] found that the drag force is much less when active swimming than passive swimming. Liu [5] adopted Quasi vortex lattice method to calculate the propulsive efficiency.

In order to control the movement of robotic dolphins, it is very significant to study the dynamic modeling. In general the propulsion mechanism consists of a series of multiple rigid joints, and the fins are made of elastic skeleton or flexible material to enhance flexibility and reduce water drag. Therefore, the propulsion mechanism is usually regarded as a multi-body dynamics system. Presently, there are four types of common multi-body dynamics methods commonly used, namely the Newton–Euler

* Corresponding author. Tel.: +86 01068915616.
E-mail address: 35146627@qq.com (G. Ren).

http://dx.doi.org/10.1016/j.robot.2015.07.014
0921-8890/

method [6,7], Lagrangian method [8], Schiehlen method [9,10] and Kane method [11]. By applying these methods, numerous representative results have been achieved in recent years, as follows. Zhou [12] adopted the Lagrangian method to study the dynamic model of one-joint thunniform robotic fish, in which water dynamics were analyzed by the resistance model. Shen [13] adopted the Kane method to establish a dynamic model for robotic dolphins, in which the dynamic analysis of wave movement was simplified, and further generalized that the inertial force and generalized active force are used to build dynamic equation. Yu [14,15] used the Schiehlen method to obtain the dynamic model for robotic dolphins and robotic fish in three-dimensional water space, and applied the model to obtain three-dimensional swimming curves in simulation.

In terms of movement control implementation, there have been few research results for robotic dolphins. Nakashima [16] realized the pitch maneuver by controlling the propulsive joints, and realized yaw and roll maneuvers by controlling the dorsal fin and pectoral fin. Simulations and experiments were performed by PID policy. Yu [17] realized propulsive speed control through studying the oscillating frequency and amplitude of the tail, and yaw control through controlling turning joints. The main achievement of the above two studies is open loop control without a feedback loop. Wang [18] presented a locomotion controller by using the Central Pattern Generator (CPG) model with nearest coupling for a multi-jointed robotic dolphin, and realized propulsion and maneuver for robotic dolphins. Shen [19] proposed a fuzzy PID controller to realize depth control by considering the nonlinear model in the depth control and volume variation of the rubber skin due to water pressure. Wang [20] gives a modeling and open loop control method, in which the robotic dolphin is modeled as a three segment organism. That is a rigid anterior body, flexible rear body, and an oscillating fluke. The dorsoventral movement generates the thrust, and bending of the anterior body in the horizontal plane enables turning maneuvers.

The above studies are very useful for further research of robotic dolphin. At the same time, they also show that the dynamic modeling is a complex issue. In particular, the existing model seldom is applied to conduct robotic dolphin movement in aquatic environments. Due to the complexity and fluidity of water, these models, which are based on multi-body dynamics method, become seriously distorted and are not suitable for application.

For the purpose of obtaining practical kinematic model and converting the speed control issue into a kind of pure control problem, this study attempts to find a data-driven way to propel the robotic dolphin. First, it proposes a KEMC definition based on the kinetic energy mapping feature and obtains a KEMC feature equation. Then it designs an average propulsive speed control method by applying the KEMC equation. Among them, parameter iterative identification and adaptive control method are adopted respectively. Simulation analysis and experimental results show that the feature data KEMC could be used to direct the robotic dolphin's motion, and the speed control implementation approach is feasible.

2. Kinematic feature descriptions and extraction methods

2.1. Kinematic features

On the basis of the biological observations of dolphin swimming, Romanenko [21] established Eq. (1) to describe the periodic excursions of the body centerline in dorsoventral movements:

$$h(x_n, t) = h^T f(x_n) \sin \omega t \tag{1}$$

where h^T denotes the maximal vertical excursion of the fluke; BL denotes the body's length of the dolphin; $x_n = x/BL$ represents the longitudinal coordinate, which is measured from the rostrum, divided by the BL; $f(x_n)$ is the polynomial expression of x_n; ω is the angle velocity; and t is time.

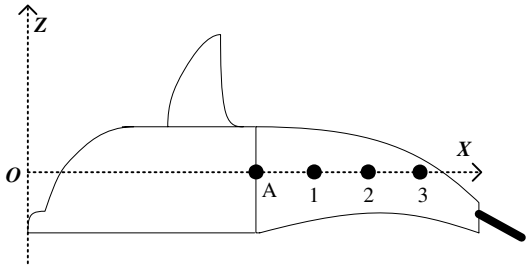

Fig. 1. The oscillating tail with three centroids.

A large number of observations show that, when a dolphin continues to oscillate on a certain frequency and amplitude of tail, it will obtain a corresponding forward speed. Once the aquatic environment is stable, the average speed will remain changeless after a few 2π oscillating periods of tail.

Eq. (1) describes the body centerline oscillating rule for the dorsoventral movements of dolphins. Every point on the centerline oscillates on a sinusoidal wave. In Fig. 1, Point A represents the fixed point between tail joint and body, and point 1, points 2 and 3 represent the centroids of three joints.

In Eq. (1), when h^T and f are constants, the oscillating sinusoidal rule of the tail is changeless. From the angle of aquatic dynamics, the propulsive force of the tail is regular and stable. According to Newton's Law, the robotic fish will first accelerate, then enter a stable speed state at this moment of equilibrium of propulsive force and drag force. It is needed to point out that, although the instantaneous propulsive speed is a slightly sinusoidal fluctuation in a 2π oscillating cycle, the average propulsive speed will remain stable.

2.2. Kinetic energy mapping relation

In order to describe the kinematic features specifically, the energy conversion feature of dolphins is further analyzed.

When the dolphin is swimming at a stable state, the biological energy system is working by means of the oscillating of the tail. The biological energy is converted into three main parts: propulsive kinetic energy, kinetic energy of the surrounding water, and thermal energy. The energy conversion feature is extracted to describe the kinematic features discussed in Section 2.1. Correspondingly, a regular mapping relation exists between the kinetic energy of the tail and the propulsive kinetic energy of robotic dolphin. By sampling the representative kinetic energy of the tail in a 2π oscillating period and the average propulsive kinetic energy of the dolphin at the same moment, a mathematical equation would be obtained to describe the kinematic features. Therefore, a feature kinetic energy is defined to obtain the representative kinetic energy of the tail as shown below:

Definition 1. Feature kinetic energy.

When the dolphin's tail oscillating coincides with the X-axis, as shown in Fig. 1, the oscillating angle velocity reaches the maximum value in a 2π oscillating period. At the same time, the tail's kinetic energy also reaches the maximum value. It defines the tail's kinetic energy at this moment of $t = n\pi$ as the feature kinetic energy, which is denoted as T.

Based on the feature kinetic energy, a KEMC definition should be proposed to extract the kinematic feature for the robotic dolphin's forward motion.

2.3. Definition of KEMC

Yanov [22,23] offered the wave function on the basis of experiments, in which *Tursiops truncatus* swam at the speed of 3.12 m/s.

$$f(x_n) = 0.21 - 0.66(x_n) + 1.1(x_n)^2 + 0.35(x_n)^8. \tag{2}$$

Eqs. (1) and (2) describe the periodic excursions of the body centerline in dorsoventral movements. For the convenience of engineering applications, $f(x_n)$ is simplified as Eq. (3), based on a polynomial fit of typical dolphin-like swimming features [20,24].

$$f(x_n) = 0.1 - 1.3x_n + 2.2x_n^2. \tag{3}$$

When $x_n = 0.5, f(x_n) = 0$, it is signified that the latter half of the body is used to generate propulsive force through oscillating. It adopts three joints to fit the periodic dorsoventral movements, and the first joint is fixed at the point of $x_n = 0.5$, as shown in Fig. 1. The fluctuations of the three joints are described as follows:

$$\begin{cases} h(x_1, t) = h^T f(x_1) \sin \omega t \\ h(x_2, t) = h^T f(x_2) \sin \omega t \\ h(x_3, t) = h^T f(x_3) \sin \omega t. \end{cases} \tag{4}$$

In Eq. (4), x_1, x_2 and x_3 represent the longitudinal coordinate of the joints' centroids, as shown in Fig. 1. The linear speed is obtained by differentiating Eq. (4), as follows:

$$\begin{cases} v(x_1, t) = 2\pi f h^T f(x_1) \cos \omega t \\ v(x_2, t) = 2\pi f h^T f(x_2) \cos \omega t \\ v(x_3, t) = 2\pi f h^T f(x_3) \cos \omega t. \end{cases} \tag{5}$$

Definition 2. KEMC.

When both the tail's oscillating frequency and amplitude are changeless, the robotic dolphin will enter a stable forward state after enough time. It samples the average propulsive speed at a stable swimming state, and defines the ratio of the average propulsive kinetic energy of the robotic dolphin to the feature kinetic energy of the three joints as KEMC, which is denoted as P.

The KEMC may be directly determined by some factors, such as the inherent physical characteristics of the robotic dolphin, as well as the steady water environment and propulsive speed of the robotic dolphin.

As a result of the KEMC definition, the basic kinetic energy mapping feature equation is as follows:

$$\frac{1}{2} M V^2(t) = P(t) T(t) \tag{6}$$

where M is the mass of the robotic dolphin; $V(t)$ is the sampled average propulsive speed; $P(t)$ is the sampled KEMC value, and $T(t)$ is the feature kinetic energy at the moment of $\omega t = n\pi, n \in N$.

3. KEMC feature equations in engineering

3.1. Engineering kinematic model

In engineering application, the servomotor is usually controlled by PWM pulse, which originates from the controller, where the duty ratio of PWM is matched with the amplitude angle of the servomotor. Therefore, the amplitude angle kinematic form of joint is needed, and usually expressed as follows [25,26]:

$$\theta(t) = \theta_{\max} \sin(\omega t) \tag{7}$$

where $\theta_{\max}$ is the maximum amplitude angle for the oscillating joint, and ω is equal to $2\pi f$. The angular velocities for the rotating body are commonly calculated as follows:

$$\dot{\theta}(t) = v(t)/r \tag{8}$$

where $\dot{\theta}(t)$ is the angle velocity. It is respectively calculated that:

$$\begin{cases} \dot{\theta}_1(t) = v(x_1, t)/r_1 \\ \dot{\theta}_2(t) = v(x_2, t)/r_2 - v(x_1, t)/r_1 \\ \dot{\theta}_3(t) = v(x_3, t)/r_3 - v(x_2, t)/r_2 \end{cases} \tag{9}$$

where r_1, r_2, r_3 are respectively the centroid radii of the gyrations for the three joints, and $r_i = (2i - 1)L/2$ when $\theta_i = 0, i = 1, 2, 3$. The integral of Eq. (9) is as follows:

$$\begin{cases} \theta_1(t) = 2h^T f(x_1) \sin \omega t / L \\ \theta_2(t) = 2h^T f(x_2) \sin \omega t / 3L - 2h^T f(x_1) \sin \omega t / L \\ \theta_3(t) = 2h^T f(x_3) \sin \omega t / 5L - 2h^T f(x_1) \sin \omega t / 3L. \end{cases} \tag{10}$$

Eq. (10) gives the amplitude angle form of Eq. (4) at the moment of $\omega t = n\pi$. Fig. 2 gives the changing amplitude angle $\theta_i(t)$ of the three joints. Notably, there is no phase difference between two adjacent joints.

3.2. Feature kinetic energy T

According to the definition of KEMC, the feature kinetic energy of the three oscillating joints should first be calculated. Eq. (10) offers the amplitude angle kinematic equations. According to Definition 1 and the Lagrange equation, when $\omega t = n\pi, n \in N$, direct calculation gives the following [12,27]:

$$T_i(t) = \frac{1}{2} m v^2(x_i, t) + \frac{1}{2} J_i \sum_{n=1}^{i} \dot{\theta}_n^2(t), \quad i = 1, 2, 3 \tag{11}$$

where

$$J_i = \frac{1}{12} m r_i \tag{12}$$

$$r_i = \frac{2i - 1}{2} L \tag{13}$$

where $T_i(t)$ is the feature kinetic energy of the ith joint; m is the mass of one joint; $v(x_i, t)$ is respectively the mass centroid linear speed of the joints; and J_i is respectively the mass centroid moments of inertia.

By calculating Eq. (11), we obtain the following:

$$\begin{cases} T_1(t) = \left(\frac{m}{2} + \frac{m}{12L}\right) f^2(x_1) \left[\frac{h^T}{\theta_{\max}}\right]^2 \omega^2(t) \\ T_2(t) = \left[\frac{m}{2} f^2(x_2) + \frac{m}{3L} f^2(x_1) + \frac{m}{36L} f^2(x_2) \right. \\ \qquad \left. - \frac{m}{6L} f(x_1) f(x_2)\right] \left(\frac{h^T}{\theta_{\max}}\right)^2 \omega^2(t) \\ T_3(t) = \left[\frac{m}{2} f^2(x_3) + \frac{m}{3L} f^2(x_1) \right. \\ \qquad + \frac{8m}{27L} f^2(x_2) - \frac{m}{6L} f(x_1) f(x_2) \\ \qquad \left. + \frac{m}{60L} f^2(x_3) - \frac{m}{18L} f(x_2) f(x_3)\right] \left(\frac{h^T}{\theta_{\max}}\right)^2 \omega^2(t). \end{cases} \tag{14}$$

3.3. KEMC feature equation

According to Definition 2, the KEMC feature equation is as follows:

$$\frac{1}{2} M V^2(t) = P(t)[T_1(t) + T_2(t) + T_3(t)] \quad t = n\pi, n \in N. \tag{15}$$

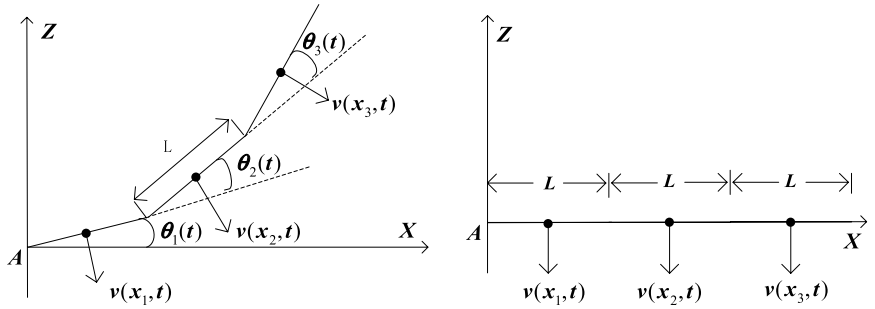

(a) The oscillating situation of three joints. (b) The oscillating situation of $\theta_i(t) = 0$.

Fig. 2. The amplitude angle changing of three joints.

Aiming at the dorsoventral movement described in Eqs. (1) and (4), according to Eqs. (14) and (15), we may calculate the KEMC feature equation to obtain the following:

$$\frac{1}{2}MV^2(t) = P(t)\left[\left(\frac{m}{2}+\frac{3m}{4L}\right)f^2(x_1) + \left(\frac{m}{2}+\frac{35m}{108L}\right)f^2(x_2) + \left(\frac{m}{2}+\frac{m}{60L}\right)f^2(x_3) - \frac{m}{3L}f(x_1)f(x_2) - \frac{m}{18L}f(x_2)f(x_3)\right]\left(\frac{h^T}{\theta_{\max}}\right)^2\omega^2(t) \tag{16}$$

where the sampling moment is $t = n\pi$, $n \in N$ for feature kinetic energy, and $V(t)$ is the average speed in one sampling period.

Remark 1. The KEMC feature equation has the following characteristics:

(1) The principle of modeling is from kinetic energy mapping feature extraction, and not commonly used in mechanics and hydrodynamics previously.
(2) The KEMC feature equation, in essence, is an uncertain proportion model with a time-varying parameter, and the equation is nonlinear and simple, but it is practical for control of robotic dolphins.
(3) In Eq. (1), there are no phase differences between any two adjacent joints, thus the KEMC feature equation is obtained on the precision of no phase difference. However, it is also suitable for traveling propulsion once the corresponding feature kinetic energy T has been obtained.

4. Average propulsive speed implementation

To implement the average propulsive speed, a parameter iterative identification and adaptive control solution is designed by applying the KEMC feature equation. Now it converts Eq. (16) into iterative form to discuss the implementation issue in the iterative domain.

4.1. Adaptive controller based on parameter iterative identification

According to Definition 2, the robotic dolphin will operate repetitively in a limited interval. It selects 6 oscillating cycles as a whole operation interval to study the control realization issue. The operation interval provides sufficient time to reach stable state, as shown in Fig. 3(a).

Similarly, according to Definition 2, the final red 2π oscillating cycle would be sampled to measure the output average speed, and to calculate the KEMC value by a law of parameter iterative. The following control issues are discussed on the provision of the limited operation interval and the given sampling cycle, as shown in Fig. 3(a).

Therefore, Eq. (16) may be expressed as the following iterative form in the limited operation interval:

$$V(j,n) = \frac{h^T}{\theta_{\max}}A\sqrt{P(j,n)}\omega(j,n), \quad j \in N, n = 6 \tag{17}$$

in which

$$A = \sqrt{\left(\frac{m}{M}+\frac{3m}{2ML}\right)f^2(x_1) + \left(\frac{m}{M}+\frac{35m}{54ML}\right)f^2(x_2) + \left(\frac{m}{M}+\frac{m}{30ML}\right)f^2(x_3) - \frac{2m}{3ML}f(x_1)f(x_2) - \frac{m}{9ML}f(x_2)f(x_3)} \tag{18}$$

where j is operation iterations, and n is the sampled cycle in the operation interval, and is equal to 6. The iterative period is set at 6 oscillating cycles to ensure entering into stable state.

An adaptive control with parameter iterative identificationis then designed, as shown in Fig. 3(b).

n is a constant for the entire operation course, thus n is not mentioned for simplification of analysis in the following section.

The system error is as follows:

$$e(j) = V(j) - V_d \tag{19}$$

where $V(j)$ is the sampling speed at the stable state, and V_d is the speed target.

The laws of parameter iterative and the law of adaptive control are as follows:

$$P(j) = P(j-1) + Q(j)e(j) \tag{20}$$

$$\omega(j+1) = \frac{\theta_{\max}V_d}{h^TA\sqrt{P(j)}} \tag{21}$$

where $Q(j)$ is the iterative gain.

4.2. Issues of initial value and iterative period

(1) For the propulsive system of the three-jointed robotic dolphin, the value of h^T could theoretically be selected in the range of $[0, 3L]$.
(2) The value of $P(0)$ must be set only once in the same aquatic environment, and may be obtained by offline measurement, or be given an empirical value. The difference is that if the initial error is smaller, then the iterative time will be shorter. The initial value of $\omega(1)$ is determined by $P(0)$ and the control target V_d.
(3) The limited operation interval must ensure that the robotic fish may enter a stable state. It is preliminarily set to 6 oscillating cycles, thus the iterative operation period is $12\pi/\omega(j)$.

Remark 2. The adjustment of the target speed is gradually completed through several iterative periods, so that every iterative unit's time is different according to the changing signal $\omega(j)$.

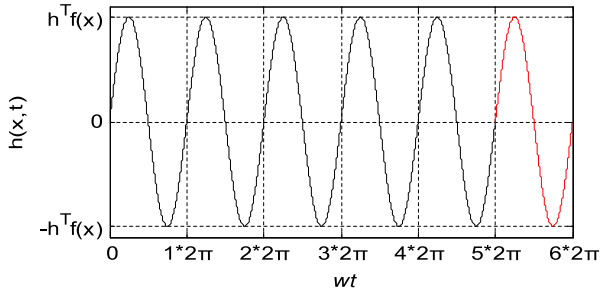

(a) Tail oscillating in a whole operation interval.

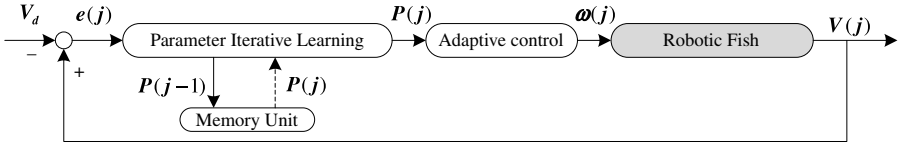

(b) Adaptive control with parameter iterative identification.

Fig. 3. Implementation of average speed control. (For interpretation of the references to color in this figure legend, the reader is referred to the web version of this article.)

4.3. Analysis of convergence

Theorem 1. *The system, which consists of model (17), law of adaptive control (20) and law of parameter iterative (21), has the following characteristics:*

(1) *All parameters and signals in the system are bounded.*
(2) *In the iterative domain, when* $j \to \infty$*, the system error approaches zero:*

$$\lim_{j\to\infty} e(j) = 0, \quad j \in N. \tag{22}$$

Proof. (1) The initial value $\boldsymbol{P}(0)$ is given as a constant by offline identification in advance, and according to Eq. (20), the $P(j)$ would be monotonous by designing a suitable parameter learning gain $Q(j)$. Suppose that the actual $\boldsymbol{P}_0$ is less than $\boldsymbol{P}(0)$, thus the supremum of $P(j)$ is $\boldsymbol{P}(0)$, and the infimum of $P(j)$ is $\boldsymbol{P}_0$. The $P(j)$ would be Monotonic decrease by designing a suitable parameter learning gain $Q(j)$. According to the Theorem of Nested Interval, if the series exist a supremum or infimum, the monotonous series should be bounded. Thus, the $P(j)$ is bounded. Similarly, if the actual $\boldsymbol{P}_0$ is greater than $\boldsymbol{P}(0)$, thus the supremum of $P(j)$ is $\boldsymbol{P}_0$, and the infimum of $P(j)$ is $\boldsymbol{P}(0)$. The $P(j)$ would be Monotonic increase by designing a suitable parameter learning gain $Q(j)$, thus, the $P(j)$ is bounded.

For $\omega(1) = \theta_{\max} V_d/(h^T A\sqrt{P(0)})$, thus the $\omega(1)$ is a bounded initial value. For the law of adaptive control $\omega(j+1) = \theta_{\max} V_d/(h^T A\sqrt{P(j)})$, a suitable learning gain $Q(j)$ may be designed to make $\mathrm{Lim}_{j\to\infty}\omega(j+1)$ approach the stable value monotonically. Therefore, the $\omega(j+1)$ is bounded between the initial value and stable value. Similarly, the output signal is bounded due to Eq. (17) by the actual P_0.

(2) The jth iterative error equations is

$$e(j) = V(j) - V_d. \tag{23}$$

The actual output signal is

$$V(j) = \omega(j)\frac{h^T}{\theta_{\max}} A\sqrt{P_0} \tag{24}$$

where the P_0 is the actual KEMC at stable state. According to Eq. (21), the input signal is

$$\omega(j) = \frac{\theta_{\max} V_d}{h^T A\sqrt{P(j-1)}}. \tag{25}$$

Substituting Eqs. (24) and (25) into Eq. (23), we obtain the following:

$$e(j) = \left(\frac{\sqrt{P_0}}{\sqrt{P(j-1)}} - 1\right) V_d. \tag{26}$$

According to Eq. (20):

$$P(j-1) = P(j-2) + Q(j-1)e(j-1). \tag{27}$$

Case 1: $P(j-1) \geq P_0, j \in N$.

For $P(j-1) \geq P_0$, so $e(j) \leq 0$. A suitable iterative gain is designed as follows:

$$Q(j-1) = \frac{\rho P(j-2)}{V_d}, \quad 0 \leq \rho \leq 1. \tag{28}$$

Substituting Eq. (28) into Eq. (27) yields the following:

$$P(j-1) = P(j-2) + P(j-2)\frac{e(j-1)\rho}{V_d}. \tag{29}$$

The $e(j-1) \leq 0$ and other parameters are not negative, thus the $P(j-1)$ will be monotone decreasing. Considering the range of $P(j-1)$ is $[P_0, P(0)]$, and according to the Theorem of Nested Interval, the following is true:

$$\lim_{j\to\infty} P(j-1) = P_0, \quad j \in N. \tag{30}$$

Correspondingly, according to Eq. (26), the following is also true:

$$\lim_{j\to\infty} e(j) = 0. \tag{31}$$

Case 2: $P(j-1) \leq P_0, j \in N$.

For $P(j-1) \leq P_0$, thus $e(j) \geq 0$. Similarly, a suitable iterative gain is designed as follows:

$$Q(j-1) = \frac{\rho P(j-2)}{V_d}, \quad 0 \leq \rho \leq 1. \tag{32}$$

Substituting Eq. (32) into Eq. (27) yields the following:

$$P(j-1) = P(j-2) + P(j-2)\frac{e(j-1)\rho}{V_d}. \tag{33}$$

The $e(j-1) \geq 0$ and other parameters are not negative, thus the $P(j-1)$ would be monotone increasing. Considering the range of

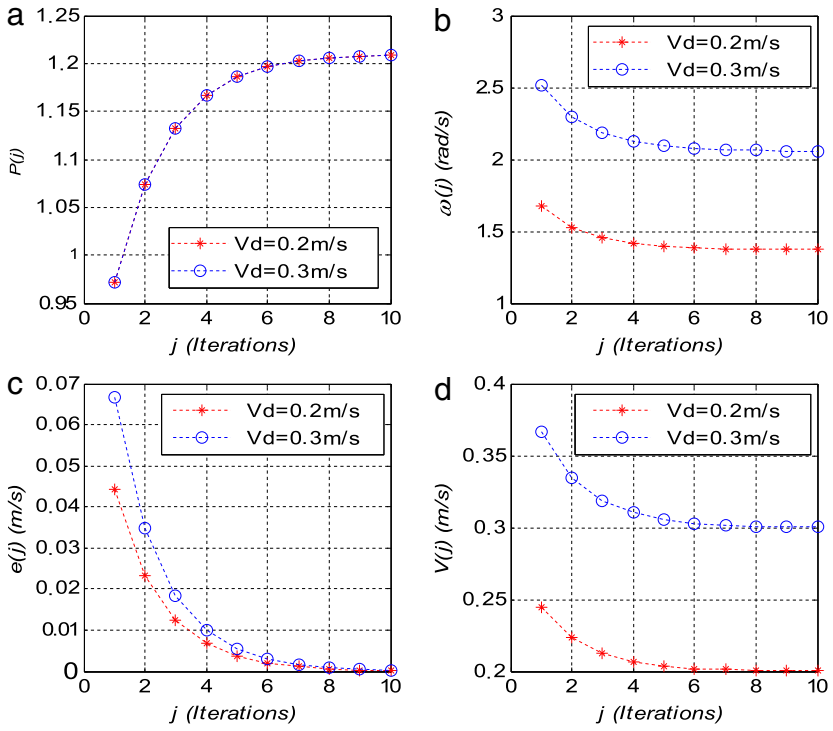

Fig. 4. (a) Identification curves of parameters. (b) Input angle velocity. (c) Output propulsive speed. (d) Error convergence curves. (For interpretation of the references to color in this figure legend, the reader is referred to the web version of this article.)

$P(j-1)$ is $[P(0), P_0]$, and according to the Theorem of Nested Interval, the following is true:

$$\lim_{j\to\infty} P(j-1) = P_0, \quad j \in N. \tag{34}$$

Correspondingly, according to Eq. (26), we obtain the following:

$$\lim_{j\to\infty} e(j) = 0. \tag{35}$$

According to the results of cases 1 and 2, the speed control system is convergent in the iterative domain. This completes the proof.

5. Simulation analysis

According to the inherent physical characteristics of robotic fish, the parameters are set in Eq. (17) to $m = 0.3$ kg; $M = 10$ kg; $L = 0.1$ m; $h^T = 0.2$ m; $\boldsymbol{\theta}_{\max} = 0.588$ rad, and the parameters in Eq. (3) are set to $x_1 = 0.5833$ $x_2 = 0.75$ $x_3 = 0.9167$. Therefore the KEMC feature equation is as follows:

$$V(j) = 0.0785\sqrt{P(j)}\omega(j). \tag{36}$$

5.1. Speed adjustment

We set $P = 1.21$ and $P(0) = 0.81$, where P is the actual KEMC when the robotic fish is in the current aquatic environment. The parameter learning gain is designed as follows:

$$Q(j) = \frac{0.99P(j-1)}{V_d}. \tag{37}$$

The iterative period is also set to 6 oscillating cycles. The simulation results are shown in Fig. 4.

For the velocity targets 0.2 m/s and 0.3 m/s, Fig. 4(a) gives the iterative course for the coefficient $P(j)$, and the value of $P(j)$ iteratively increases from 0.81 to the stable value of 1.21. On different speed targets, the iterative tracking is basically consistent.

Table 1
Iterative operation time and error.

Iteration number	Time (s)	Error
1	13.32	0.045
2	14.6	0.022
3	15.31	0.013
4	15.75	0.007
5	16	0.003
6	16.1	0.002
7	16.14	0.001
8	16.2	∼0

Fig. 4(b) shows that the input signals $\omega(j)$ successively decrease from the initial values of 2.5 rad/s and 1.7 rad/s to the stable values of 2.1 rad/s and 1.4 rad/s, which are the respective oscillating angular velocities under the target propulsive speeds of 0.2 m/s and 0.3 m/s. Converting into frequency, the final oscillating frequencies are respectively 0.9 times per second and 1.35 times per second. This shows that the input signal $\omega(j)$ will reach a stable value along with the precise identification of $P(j)$.

Fig. 4(c) and (d) show the adjustment results of the speed control. It is shown that the velocity error basically converges to 0 m/s along with the final inputting signal $\omega(10)$.

For the two target velocities of 0.2 m/s and 0.3 m/s, although the initial errors $e(j)$ are different, the convergence performance is basically consistent. This shows that the law of control and law of parameter iterative have determined the system's convergence.

The sampling iterative period is 6 oscillating cycles, thus the iterative time is $t(j) = 12\pi/\omega(j)$ for the jth iterative operation. All ten iterative operation times for the target speed of 0.2 m/s are listed in Table 1.

At the seventh iteration, the speed's error is 0.001 m/s, which is less than 1%. The total iterative operation time at this moment is 107.1 s. This shows that the robotic fish will basically reach a target speed state in 107.1 s, and that the actual P value is identified.

Remark 3. 107.1 s is a relatively long time, but this is only for the first operation, the following switching course requires much less

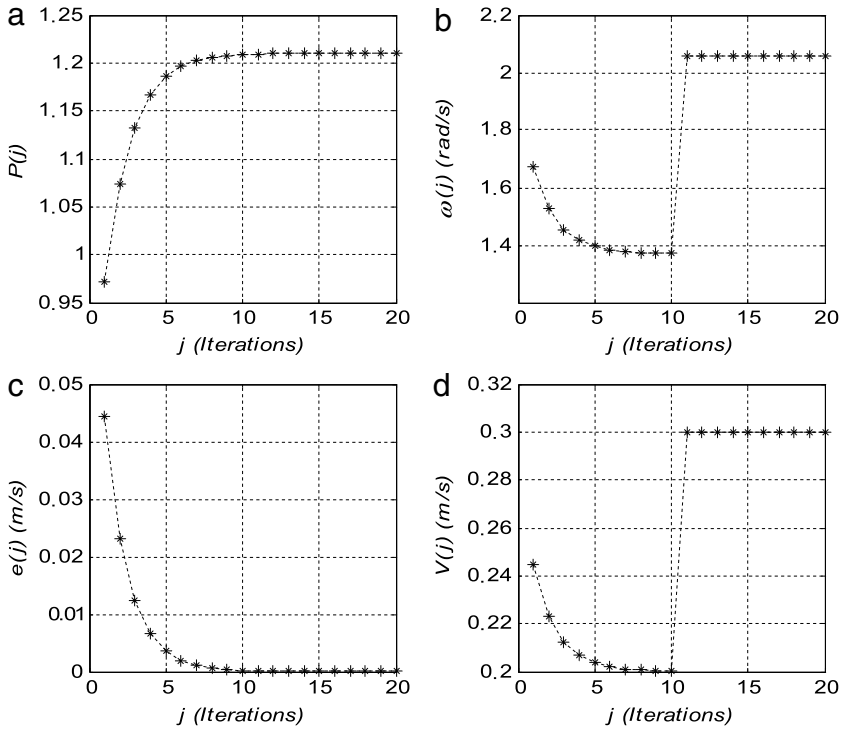

Fig. 5. (a) Switching of parameter. (b) Switching of input angle velocity. (c) Speed adjustment. (d) Error convergence curve.

time. More importantly, monotone successive approaching will ensure the stability of the KEMC value. In addition, the discussed speed adjustment method is mainly suitable for long distance swimming application.

5.2. Speed switching

When $V_d = 0.2$ m/s switches to 0.3 m/s at the eleventh iteration, and the switching curves are as shown in Fig. 5.

When the target speed switches from 0.2 m/s to 0.3 m/s at the eleventh iteration, we can see from Fig. 5(a) that the $P(j)$ undergoes no change. The previous ten iterative operations have correctly identified the actual KEMC value, so that the actual value may be selected as an initial value when switching. At the moment of the eleventh iteration, the control system acquires the actual $P(10)$ value and quickly realizes the adjustment of input angle velocity, and the output speed and error both reach to zero at the same time, as shown in Fig. 5(c) and (d). Fig. 5(d) shows that the speed error undergoes no change at the switching point.

As a result, the eleventh iteration time is 10.85 s, thus the robotic fish will reach 0.3 m/s in 10.85 s, thereby greatly reducing the time compared with the first operation. Similarly, switching of the later target speeds will also perform in this manner.

Therefore, the value of the KEMC is stable in the same aquatic environment, once the KEMC is identified at the first target speed it may be used for the follow-up control target, and the speed adjustment will be much faster than the first target operation.

6. Experiments

The simulations theoretically prove the feasibility of the average speed control. Physical experiments would also be carried out to further verify the effectiveness of average speed control. To ensure the convergence of speed on the experiment, the initial KEMC value should be close to the actual value. Thus the experiment is divided into two parts, offline identification of the initial KEMC value, and closed loop control.

Table 2
Physical parameters of robotic dolphin.

Size (L ∗ W ∗ H)	80 ∗ 36 ∗ 24 cm
Length of tail	38 cm
Size of caudal fin (L ∗ W)	7 ∗ 20 cm
Length of joint	10 cm
Mass of fish body	9 kg
Quantity of servomotors	3
Mass of servomotor	0.08 kg
Mass of one joint	approx. 0.3 kg
Time of battery life	approx. 2 h
Communication mode	Wireless (435.92 MHz)
Speed measurement	Ultrasonic
$\boldsymbol{h}^T$	0.2 m
$\boldsymbol{\theta}_{\max}$	0.588 rad

6.1. Robotic dolphin prototype

A robotic dolphin prototype is designed, as shown in Fig. 6. Three servomotors are in series and generate a propulsive force by regular oscillating. As a whole propulsive system, a flexible crescent caudal fin is fixed with the last joint.

The physical parameters of the robotic dolphin are listed in Table 2.

A 10 m long swimming pool is used to carry out the experiment.

6.2. Offline identification of KEMC

For the KEMC feature equation, the parameters are the same as the simulation case, so that the KEMC feature equation is equally calculated as follows Eq. (36).

A series of $\omega(j)$ is respectively inputted and the corresponding propulsive average speed is measured. As a result, a database of KEMC is obtained by offline identification. Offline identification is carried out for three times repeatedly in 5 m distance, and the average speed is measured by artificial way. The experimental scene is shown in Fig. 7.

Eq. (36) is used to calculate the KEMC value, the identification results are shown in Table 3.

Table 3
Offline identification results.

$\omega(j)$ (rad/s)	0.56π	1.11π	1.67π	2.22π	2.78π	3.33π	3.89π	4.45π	5π	5.56π
$V(j)$ (m/s)	0.04	0.08	0.13	0.18	0.23	0.28	0.33	0.38	0.29	0.21
$P(j)$	0.084	0.087	0.1	0.108	0.113	0.116	0.118	0.12	0.055	0.023

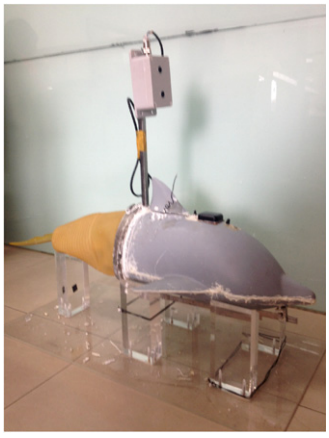

Fig. 6. Experimental robotic dolphin.

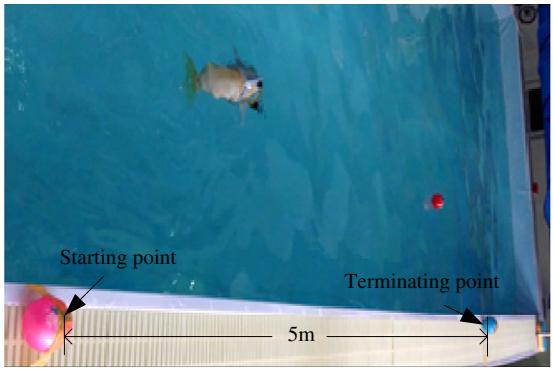

Fig. 7. KEMC and average speed at stable state.

According to Table 3, Fig. 8(b) gives the KEMC's distribution with the increase of speed.

We can see from Table 3 and Fig. 8 that every input angle velocity has a corresponding KEMC value in the current aquatic environment for the robotic dolphin with feature equation, and the KEMC value is basically stable.

When the angle velocity is 4.45π rad/s, the KEMC reaches the maximum value, signifying the highest energy conversion efficiency. When the angle is over 4.45π rad/s, the KEMC value decreases quickly, which means that the tail's oscillating enters a saturated state, and the propulsive efficiency will decrease quickly. At the same time, the KEMC feature in Eq. (36) is not suitable for conducting the robotic dolphin's movement once the angle velocity is over 4.45π rad/s.

Once the KEMC value is clear, the robotic dolphin's average speed would be obtained. KEMC data would be used to generate the angular velocity corresponding to the target speed. Theoretically, the open-loop driven could reach the target speed approximately.

For self-regulation of robotic dolphin, these eight KEMC values in Table 3 would be as the initial reference values for the closed loop speed control. Conversely, the closed loop control results would update these values in Table 3.

6.3. Closed loop speed control

Taking 0.3 m/s as a speed target, a closed loop speed control experiment is carried out. To enhance the reliability of the system, the first sampled period is designed as 2 s and the parameter learning gain is selected as follows:

$$Q(j) = \frac{0.95P(j-1)}{V_d}. \tag{38}$$

The speed is measured through two ultrasonic modules. One module is mounted on the robotic dolphin, and which would receive ultrasonic. The other is fixed in the front of robotic dolphin, and which would transmit ultrasonic. The motion speed is calculated by measure the change of distance. The transmitting period is 443 ms, and the sampling period is 2 s. The closed four measured speed values are used to calculate the average speed $\boldsymbol{V}$. Fig. 9 gives the experimental scene.

The experiment is repeatedly carried out for 5 times, and the swimming effectiveness is basically similar. Fig. 10 gives the operation data at one time.

For reducing errors and improving the data reliability, the measured $V(j)$ is filtered by a threshold interval of [0.285, 0.315]. All measured data would be regarded as invalid once over the threshold interval, and this ensures that the control system is verified successfully. We can see from Fig. 10(b), the third data is invalid, and the fourth, the eighth data are also invalid. In Fig. 10(a), the KEMC value is not adjusted because of the invalid speed data.

In Fig. 10(a), the stable KEMC value is identified as 0.117 for the target speed 0.3 m/s. Compared with the simulation course, the physical robotic dolphin may reach a close speed value more quickly because of the close initial KEMC value 0.116 in Table 3. The experimental results prove further that the KEMC data could be used to propel the robotic dolphin, and the closed loop control could identify the KEMC value more detail.

6.4. Comparison analysis

The propulsive speed implementation approach is different with the past typical researches which are shown in papers [17,18]. The following is the detailed comparison.

An OscData[M][N] array is proposed to drive the robotic dolphin. There are a few significant differences between the OscData[M][n] and the KEMC method.

First, the OscData[M][N] is forecasted by given $\boldsymbol{h}^T$, and it is a constant; but the KEMC is an uncertain parameter, and the initial value should be identified offline. In essence the KEMC is a dynamic data. Second, an open loop control is implemented in [17] by applying OscData[M][N], but the KEMC method implements the closed loop control based on external feedback. Most importantly, the speed errors are different. The OscData[M][N] method could forecast the data, but cannot revise the data, so larger error appear in [17]. But for KEMC method, the initial P value is closed to an actual value, so error is much less, and further, the KEMC has learning ability.

A CPG model is adopted to propel the robotic dolphin in [18]. A series of CPG parameters are set to get a measured speed. Similar to OscData[M][N] method, it propels the robotic dolphin, but does not control the robotic dolphin. The KEMC method has less error in open loop control, furthermore, the robotic dolphin obtains learning and adaptability in closed loop control. The dynamic characteristic of KEMC is the key of learning and adaptability.

Totally, the KEMC method has obvious advantages: dynamic data, closed loop control, learning ability and adaptability.

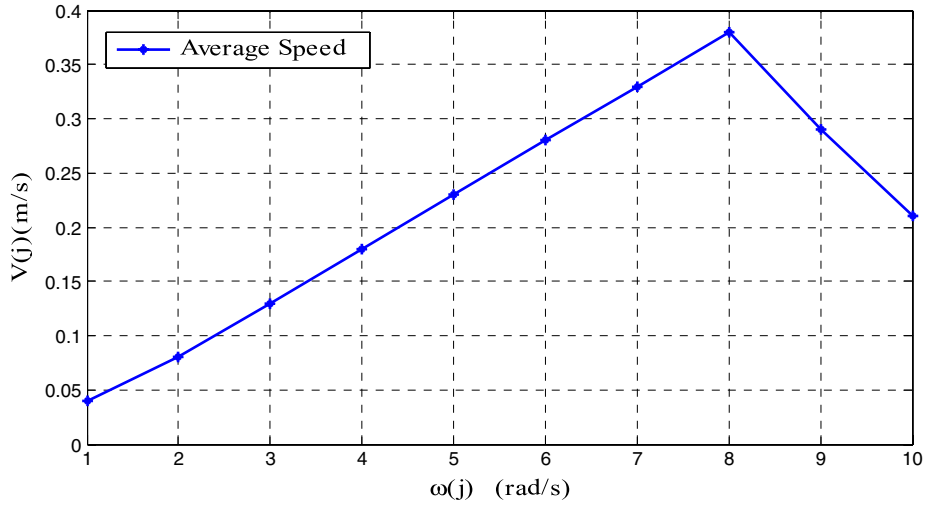

(a) The measured average speed value.

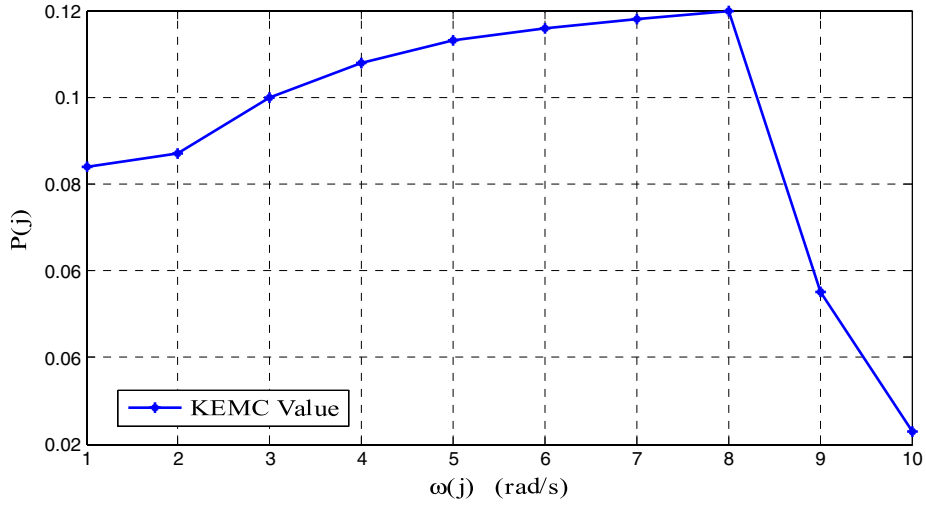

(b) The identification of KEMC.

Fig. 8. KEMC and average speed at stable state.

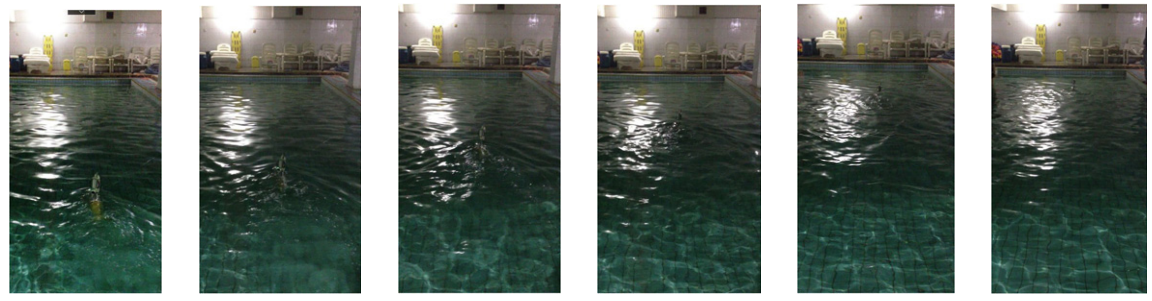

(a) 2 s. (b) 4 s. (c) 8 s. (d) 12 s. (e) 16 s. (f) 20 s.

Fig. 9. Experimental scene for closed loop control.

7. Conclusions

This paper proposed a systematic solution based on KEMC for the robotic dolphin's propulsion both theoretically and experimentally. It offers two main distributions for average speed implementation of robotic dolphins with multi-joint propulsion, as follows.

One, the feature extraction method is introduced to analyze the kinematics of robotic dolphins, which is also suitable for BCF robotic fish with caudal fin propulsion, and a KEMC is defined on the basis of extracting kinetic energy mapping features.

Second, parameter iterative learning and adaptive control are applied to realize the speed control of robotic dolphins by using the KEMC data, thereby exploring a data-driven approach for robotic dolphin' average speed implementation.

Further research objectives include the whole identification of KEMC for a certain robotic dolphin without physical and environmental changes, and establish a more detailed datasheet

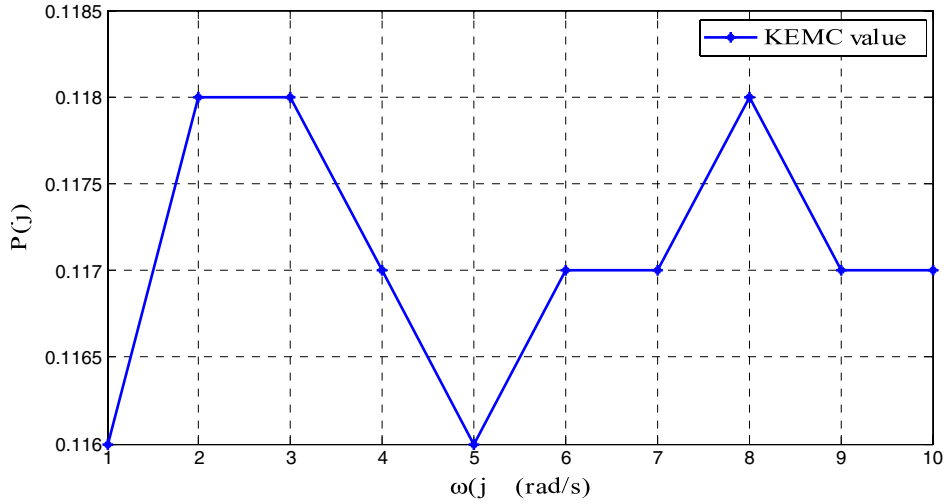

(a) The runtime values of KEMC.

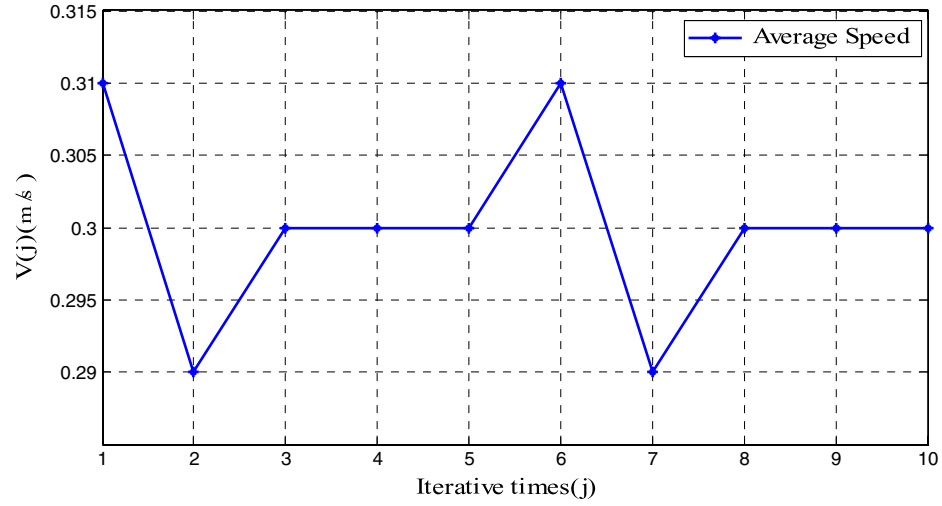

(b) The measured values of average speed.

Fig. 10. The average speed adjustment process.

for different average speed targets. Second, the optimization of the control system should be carried out in terms of three aspects, namely shortening the speed adjustment time, strengthening the anti-disturbing ability, and enhancing the energy conversion efficiency. Besides, the KEMC could be an evaluating indicator for propulsion efficiency research.

References

[1] N. Bose, J. Lien, Propulsion of a fin whale (Balaenoptera physalus): why the fin whale is a fast swimmer, Proc. R. Soc. Lond. Ser. B 237 (1989) 175–200.
[2] M. Nakashima, A simple calculation method to analyze the dynamics of carangiform propulsion, in: Proceedings of the International Symposium on UUS Technology, 1999, pp. 320–329.
[3] D. Weihs, The hydrodynamics of dolphin drafting, J. Biol. 3 (8) (2004) 1–16.
[4] D.S. Barrett, M.S. Triantafyllou, D.K.P. Yue, M.A. Grosenbaugh, M. Wolfgang, Drag reduction in fish-like locomotion, J. Fluid Mech. 392 (1999) 183–212.
[5] P. Liu, N. Bose, Propulsive performance of three naturally occurring oscillating propeller planforms, Ocean Eng. 20 (1993) 57–75.
[6] W. Khalil, G. Gallot, F. Boyer, Dynamic modeling and simulation of a 3-D serial eel-like robot, IEEE Trans. Syst. Man Cybern. Part C Appl. Rev. 6 (2007) 1259–1268.
[7] F. Boyer, M. Porez, A. Leroyer, M. Visonneau, Fast dynamics of an eel-like robot comparisons with Navier–Stokes simulations, IEEE Trans. Robot. 24 (6) (2008) 1274–1288.
[8] T.Q. Vo, H.S. Kim, B.R. Lee, Propulsive velocity optimization of 3-joint fish robot using genetic-hill climbing algorithm, J. Bionic Eng. 6 (4) (2009) 415–429.
[9] W. Schiehlen, Technische Mechanik, Teubner, Stuttgart, 1986.
[10] W. Schiehlen, Multibody system dynamics: roots and perspectives, Multibody Syst. Dyn. 1 (2) (1997) 149–188.
[11] T.R. Kane, D.A. Levinson, Multibody dynamics, J. Appl. Mech. 50 (4b) (1983) 1071–1078.
[12] C. Zhou, Z. Cao, S. Wang, M. Tan, The design, modelling and implementation of a miniature biomimetic robotic fish, Int. J. Robot. Autom. 25 (3) (2010) 210–216.
[13] F. Shen, Z.Q. Cao, D. Xu, C. Zhou, The dynamic model of robotic dolphin based on Kane method and its speed optimization method, Acta Automat. Sinica 38 (8) (2012) 1247–1256.
[14] J. Yu, L. Liu, M. Tan, Three-dimensional dynamic modelling of robotic fish: simulations and experiments, Trans. Inst. Meas. Control 30 (3–4) (2008) 239–258.
[15] J. Yu, Y. Li, Y. Hu, L. Wang, Modeling and control of a link-based dolphin-like robot capable of 3D movements, in: Intelligent Robotics and Applications, in: Lecture Notes in Computer Science, vol. 5314, 2008, pp. 982–991.
[16] M. Nakashima, T. Tsubaki, K. Ono, Three-dimensional movement in water of the dolphin robot-control between two positions by roll and pitch combination, J. Robot. Mechatronics 18 (3) (2006) 347–355.
[17] J.Z. Yu, Y.H. Hu, R.F. Fan, L. Wang, J.T. Huo, Mechanical design and motion control of biomimetic robotic dolphin, Adv. Robot. 21 (3–4) (2007) 499–513.
[18] M. Wang, J. Yu, M. Tan, J. Zhang, Design and implementation of a novel CPG-based locomotion controller for robotic dolphins, in: Proceedings of the 8th World Congress on Intelligent Control and Automation, Jinan, China, 2010, pp. 1611–1616.

[19] F. Shen, Z.Q. Cao, Depth control for robotic dolphin based on fuzzy PID control, Int. J. Offshore Polar Eng. 23 (3) (2013) 166–171.
[20] J. Yu, Y. Hu, R. Fan, L. Wang, J. Huo, Mechanical design and motion control of biomimetic robotic dolphin, Adv. Robot. 21 (3–4) (2007) 499–513.
[21] E.V. Romanenko, Fish and Dolphin Swimming, Pensoft, Moscow, Russia, 2002, p. 127.
[22] V.G. Yanov, Kinematics of dolphins, new results of experimental studies, DAN SSSR 315 (1990) 49–52.
[23] V.G. Yanov, Experimental investigating kinematics of three actively swimming modes in the Black sea bottlenose dolphin (Tursiops truncatus), Usp. Sovrem. Biol. 117 (1997) 704–725.
[24] F.E. Fish, J.J. Rohr, Review of dolphin hydrodynamics and swimming performance, United State Navy Technical Report 1801, August 1999.
[25] J. Ayers, N. Rulkov, Controlling biomimetic underwater robots with electronic nervous systems, in: Bio-mechanisms of Animals in Swimming and Flying, Springer-Verlag, 2008, pp. 295–306. (Chapter 24).
[26] Jun Gao, Shusheng Bi, Yicun Xu, Development and design of a robotic manta ray featuring flexible pectoral fins, in: International Conference on Robotics and Biomimetics, December 15–18, 2007, Sanya, China, 2007, pp. 519–523.
[27] Chao Zhou, Zeng-Guang Hou, Zhiqiang Cao, Shuo Wang, Min Tan, Motion modeling and neural networks based yaw control of a biomimetic robotic fish, Inform. Sci. 237 (2013) 39–48.

Ren Guang is a Ph.D. candidate at the Beijing Institute of Technology. His research interest covers the kinematic and intelligent control of robot dolphin and fish.

Dai Yaping is a Professor at the School of Automation, Beijing Institute of Technology University. Her research interest covers motion target tracking, network-based remote control, and multi-sensor data fusion for robot.

Cao Zhiqiang is an Associate Professor at the Institute of Automation, Chinese Academy of Sciences. His research interest covers multi-robot system and biomimetic robot.

Shen Fei is an Associate professor at the Institute of Automation, Chinese Academy of Sciences. His research interest covers dynamic model and motion control of robot.